The Slow Neutron Cross Sections of Indium, Gold, Silver, Antimony, Lithium, and Mercury as Measured with a Neutron Beam Spectrometer*

WILLIAM W. HAVENS, JR. AND JAMES RAINWATER
Columbia University, New York, New York

(Received August 23, 1945)†

The variations of the slow neutron transmissions of In, Au, Ag, Sb, Li, and Hg have been investigated as a function of the time-of-flight of the incident neutrons for a 5.4-meter path by use of a neutron beam spectrometer. A method of analysis is developed for determining E_0 and $\sigma_0\Gamma^2$ for resonances above 1 ev based on the experimental transmission curves and the Breit-Wigner theory. The positions of the levels located, listed in order of importance for each element, are: In, (1.44±0.04) ev; Au, (4.8±0.2) ev; Ag, (5.11±0.2) ev, (13.7±1) ev, and (43±5) ev; Sb, (6.3±0.5) ev, (19.2±1.0) ev, and indications of other unresolved levels in the region of 50 to 500 ev; Li, only a $1/v$ cross section; Hg, a negative level at (−2.0±0.2 ev) and indications of unresolved positive levels above 25 ev. In the thermal region, the Ag, Sb and Li cross-section curves can be resolved into the sum of a constant term and a $1/v$ term. If E is the neutron energy in ev, these are: Ag: $[(9.05\pm0.10)E^{-\frac{1}{2}}+(6.6\pm0.5)]\times10^{-24}$ cm²/atom; Sb: $[(0.64\pm0.02)E^{-\frac{1}{2}}+(4.2\pm0.3)]\times10^{-24}$ cm²/atom; Li: $[(11.5\pm0.2)E^{-\frac{1}{2}}+(1.7\pm0.2)]\times10^{-24}$ cm²/atom; LiF was used in the Li measurements and a value 2.5×10^{-24} cm²/atom has been deducted for the F. The Hg cross section below 5 ev was well matched by the relation $(64\pm3)E^{-\frac{1}{2}}(1+E/2.0)^{-2}\times10^{-24}$ cm²/atom

IN a previous paper[1] a neutron beam spectrometer system for use with the Columbia University cyclotron was described and the various instrument corrections were analyzed and evaluated.

This neutron spectrometer system uses the method of arc modulation in which the accelerating voltage for the ion source arc is modulated by a bank of hard vacuum tubes controlled by elaborate electronic timing circuits. The neutron production can be confined to intervals of 10–200 microseconds out of a 1000–10,000 microsecond cycle. Neutrons slowed down in a paraffin "source" slab are detected by a BF_3 proportional counter which for most measurements is 5.4 meters from the paraffin. Excellent collimation is obtained by using extensive B_4C and Cd shields. A special selector system counts all neutrons detected and also selectively counts those detected during an adjustable time interval after the cyclotron burst.

Investigations of other problems have been made and certain improvements in the apparatus have been carried out.

APPARATUS IMPROVEMENTS

In the previous paper it was shown that with this system there was an over-all delay time of 35 microseconds involved between the cyclotron arc pulse and the detection of the highest energy neutrons when the detector was close to the source. This time delay was therefore subtracted from all timing measurements made to obtain the actual time-of-flight of the neutron over the measured path. The measurement of this time delay was made with the BF_3 counter placed in a thick B_4C shield at an effective distance of 8 cm from the paraffin source slab. The cyclotron and the detector modulation "on-times" were made as narrow as possible and the number of counts recorded by the detector were plotted as a function of the time spacing between the cyclotron arc pulse and the timed detection intervals. These measurements were made with and without a "pulse sharpener" after the "level-setter" in the detector amplifier circuit. This pulse sharpener circuit decreased the time width of the pulses sent from the level-setter to the timed counting circuit. The results of these measurements showed that there was an effective broadening of the order of 10–15 μsec. due to that portion of the neutron counter pulse width above the level-setter height when the pulse

* A Thesis submitted by William W. Havens, Jr. in partial fulfillment of the requirements for the degree of Doctor of Philosophy in the Faculty of Pure Science, Columbia University, New York. Publication assisted by the Ernest Kempton Adams Fund for Physical Research of Columbia University.

† The experimental work on this paper was completed prior to 1943, but publication was voluntarily withheld at the request of the Manhattan District until the date indicated.

[1] J. Rainwater and W. W. Havens, Jr., Phys. Rev. 70, 136 (1946).

sharpening circuit was not used after the level-setter. This broadening, due to the width of the pulses from the neutron counter, also introduces some uncertainty in the time-of-flight measurements. It should be noted that the use of the pulse sharpening circuit after the level-setter does not influence that portion of the detector pulse width between the start of the pulse and the time when the pulse reaches a height sufficient to trip the level-setter. If this portion of the pulse width is large, the over-all time delay is correspondingly increased while differences in the width for different pulses introduces an additional resolution broadening. This is true even if the pulses leaving the level-setter are made extremely sharp. This condition may be improved by sharpening the detector pulses before they reach the level-setter height. In order to accomplish this purpose the amplifier circuit was modified to "sharpen" the pulses. The input resistor of the amplifier was reduced to 5000 ohms and the time constant of the coupling circuit between the second and third amplifier stages was greatly reduced. The measurements described above were repeated with the results shown in Fig. 1. This graph shows that the delay time using the pulse sharpening circuit is now 23 μsec. while only a slight broadening to 25 μsec. was introduced when the sharpening circuit was omitted. Therefore a delay time of 25 μsec. was subtracted from all timing measurements.

A METHOD OF ANALYSIS FOR THE MEASUREMENTS OF RESONANCE ABSORPTION LEVELS AT ENERGIES ABOVE 1 ev

In the analysis of the cadmium absorption employed in the previous paper, it was found that the experimental results could be well matched to a one-level Breit-Wigner curve over an energy range wide compared to the level width. The greatest deviation between the experimental results and the theoretical curve occurred in the region of exact resonance where a method of correcting for the resolution of the instrument was applied. In this case the correction was small, amounting to about 8 percent of the total cross section assumed for the best fit to the Breit-Wigner formula.

In the present investigations measurements were made on the transmission of indium, gold, silver, and antimony, all of which are characterized by having relatively much sharper resonance levels at higher energies than the resonance level of cadmium.[2–13]

Typical forms of such experimental transmission curves can be seen in Figs. 4, 5, 7, 9, 11, and 13 where some of the results of the measurements described in this paper are presented. These transmission curves are characterized by a sharp asymmetric dip with a clearly defined minimum and a width somewhat greater than the resolution width of the instrument. The position of the minimum in the transmission curve when corrected for asymmetric effects gives the time of flight, t_0, of the resonant neutron and from this the resonant energy E_0 can be calcu-

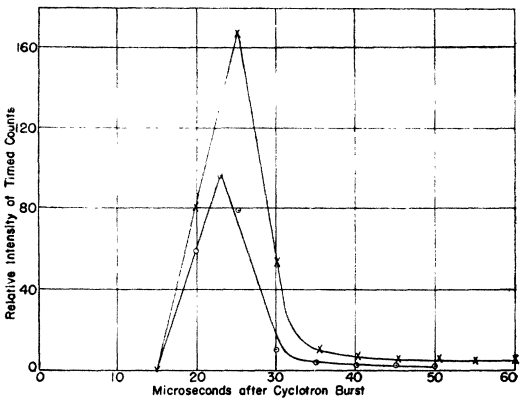

FIG. 1. Experimental resolution curve. These measurements were taken with a BF_3 counter in a thick B_4C shield with the counter axis 8 cm from the front of the paraffin source slab. The relative timed intensity is given as a function of the time between the cyclotron arc pulse and the timed detection pulse. The over-all delay time and the sharpness of the resolution are well illustrated. Circles represent the pulse sharpener in the circuit, the crosses without the pulse sharpener.

[2] H. A. Bethe, Rev. Mod. Phys. 9, 113–161 (1937).
[3] Dunning, Pegram, Fink, and Mitchell, Phys. Rev. 48, 265 (1935).
[4] Goldsmith and Rasetti, Phys. Rev. 50, 328 (1936).
[5] G. A. Fink, Phys. Rev. 50, 738 (1936).
[6] E. Amaldi and E. Fermi, Phys. Rev. 50, 899 (1936).
[7] M. Goldhaber and G. Briggs, Proc. Roy. Soc. London (A) 162, 127 (1937).
[8] H. Von Halban and P. Preiswerk, Nature, 905 (1936).
[9] H. Von Halban and P. Preiswerk, Helv. Phys. Acta 9 (318) (1936).
[10] Hornbostel, Goldsmith, and Manley, Phys. Rev. 58, 18 (1940).
[11] C. P. Baker and R. F. Bacher, Phys. Rev. 59, 332 (1941).
[12] Feeny, Lapointe, and Rasetti, Phys. Rev. 61, 469 (1942).
[13] H. Volz, Zeits. f. Physik 121, 232–234 (1943).

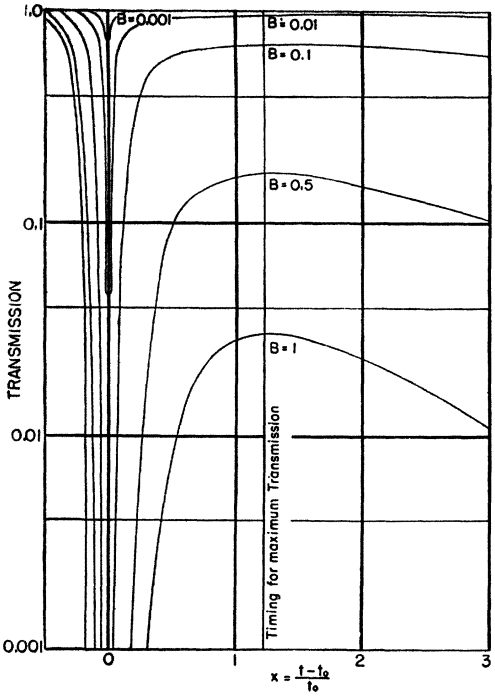

FIG. 2. Theoretical Breit-Wigner transmission curves. These transmission curves are calculated from the Breit-Wigner one-level formula using a neutron time-of-flight scale. The shapes of the curves are given for different effective sample thicknesses, $B=n\sigma_0\Gamma^2/4E_0^2$, as a function of $x=(t-t_0)/t_0$ where t_0 is the time-of-flight of a neutron at the resonance energy.

lated. If the Breit-Wigner one-level formula is assumed to hold for the cross section in the vicinity of the resonance, it is of interest to evaluate the capture cross section at exact resonance, σ_0 and the half-width of the level, Γ, as defined by the formula

$$\sigma(E)=\frac{\sigma_0\Gamma^2(E_0/E)^{\frac{1}{2}}}{\Gamma^2+4(E-E_0)^2}. \tag{1}$$

Since the experimental results are first obtained in the form of a transmission curve for the sample as a function of the time-of-flight of the incident neutrons, the most satisfactory method of analysis will be that in which the best match is made between this curve and a transmission curve calculated from the Breit-Wigner formula and corrected for the resolution effects of the instrument.

The transmission of a sample for neutrons of energy E is given by the formula

$$T_c=e^{-N\sigma(E)}, \tag{2}$$

where N=atoms/cm^2 of the absorbing material in the beam and σ is the cross section in cm^2 atom as given in formula (1).

If t represents the time-of-flight of the neutron with energy E and t_0 represents the time-of-flight for neutrons of resonant energy E_0 and we define the parameters x, λ, and B such that

$$x=\frac{t-t_0}{t_0},\quad \lambda=\frac{\Gamma}{2E_0},\quad B=N\sigma_0\lambda^2, \tag{3}$$

then the transmission of the sample as a function of these dimensionless parameters will be given by

$$T_c(x)=\exp-\frac{B(x+1)}{\lambda^2+[x(x+2)/(x+1)^2]^2}. \tag{4}$$

This dimensionless representation has certain advantages in that a table of values of

$$\frac{x+1}{\lambda^2+[x(x+2)/(x+1)^2]^2}$$

can be calculated as a function of the parameter x for several values of λ^2. Using this table of values the transmission of a sample for any value of B can be read directly from a single setting of the slide rule. Thus an easily applied system of analysis is established for the study of any resonance level at any time of flight. Also the fact that $x=0$ at exact resonance permits easier examination of the form of the function near the resonance time of flight.

In order to obtain a satisfactory dip in the experimental transmission curve when studying a sharp level, it is always necessary to choose an absorber of such a thickness that $N\sigma_0$ or B/λ^2 is large compared to unity. This corresponds to the condition that T be effectively zero at exact resonance. For values of x sufficiently far from exact resonance that T is appreciably different from zero, the λ^2 term in the denominator of the exponent is small compared to the second term in the denominator so that Eq. (3) may be replaced by the approximate relation

$$T_c=\exp\left[-B\frac{(x+1)^5}{x^2(x+2)^2}\right]. \tag{5}$$

In nuclear physics resonant absorbers are usually described as "thick" if $N\sigma_0$ is large com-

pared to unity and as "thin" if $N\sigma_0$ is small compared to unity. In the measurement of sharp levels with a neutron beam spectrometer it is always necessary that $N\sigma_0$ be large compared to unity in order to obtain a satisfactory dip in the measured transmission at resonance. Since according to the usual terminology this means that thick absorbers are always used, it is necessary to employ a different criterion for referring to the effective absorber thickness. This will be done in terms of the types of experimental transmission curves which are obtained. In Eq. (4) if $B \ll 1$ there is a sharp dip in T at exact resonance with a rapid recovery on either side of the resonant time of flight. A sample will be considered "very thin" if the recovery of T to approximately unity occurs in an interval of the same order of magnitude or smaller than the resolution width of the apparatus. If the interval between the resonant time of flight and the recovery to approximately unit transmission is larger than the resolution width of the apparatus, then the sample will be considered thin. If $0.05 < B < 0.3$ the measurements on the sample may be extended from the vicinity of resonance to the thermal energy region and the shape of the curve at energies different from the resonant energy may be studied. Samples in this region may be referred to as "medium thick." If $0.3 < B < 1$, then the sample will be referred to as thick, and if $B > 1$ then the sample will be referred to as "very thick." The thick and very thick samples are useful in studying the cross section in the region near $t = 2.2t_0$ where a maximum in the transmission curve occurs.

In Fig. 2 Eq. (3) has been plotted for five values of B with $\lambda^2 = 3 \times 10^{-3}$ illustrating the five conditions described above.

Determination of B from the Experimental Data

The area under the curve $y = (1 - T_c)$ will be given by the integral

$$F(B) = \int_a^b [1 - T(x)]dx. \qquad (6)$$

The area under this curve will be a function of the parameter B and will increase as B increases. For the purpose of this analysis the limits $x = -0.3$ and $x = 0.5$ were selected to consider only the region near the peak, where most of the effect due to the resonance occurs. It is impossible to locate the area under the total curve since as $x \to \infty$ the integral diverges due to the $E^{-\frac{1}{2}}$ factor in the Breit-Wigner formula. If the approximate value of T given by Eq. (4) is inserted in Eq. (5), the area under the curve $(1 - T)$ will be given by

$$F(B) = \int_{-0.3}^{+0.5} \left[1 - \exp\left(-B\frac{(x+1)^5}{x^2(x+2)^2}\right)\right]dx. \qquad (7)$$

The relation $F^2(B)/B$ has been plotted as a function of B in Fig. 3. This fraction approached π as B approaches zero.

Actually the area under the experimental curve $(1 - T)$ is not given accurately by the above formula because the experimental transmission at any one point is not the actual transmission of the samples at that time-of-flight but is the transmission of the sample integrated over the resolution width of the apparatus. However, it may be shown that the effect of the resolution width of the apparatus in causing the area under the experimental curve to differ from the area under the actual transmission curve is only a small edge correction. If $f(x)$ corresponding to $(1 - T_c)$ is a function whose area is confined to a region small compared to the range of integration, we may write

$$I_0 = \int_{x_1}^{x_2} f(x)dx = \int_{-\infty}^{\infty} f(x)dx. \qquad (8)$$

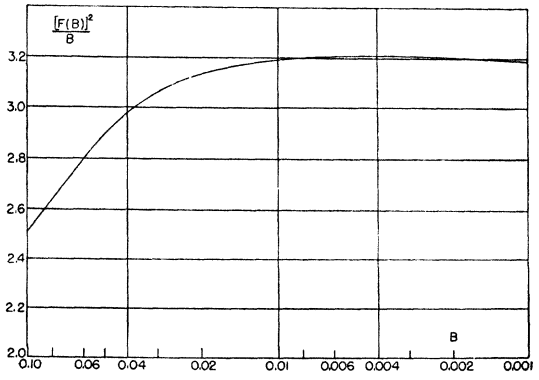

FIG. 3. Theoretical curve for determining the "effective" absorber thickness, B, from the area, $F(B)$, Eq. (7), between the experimental transmission curve and unit transmission, between the limits of $t = 0.7t_0$ and $t = 1.5t_0$. For a very thin absorber $F^2(B)/B = \pi$.

If a "smearing function" $\varphi(u)$ is now introduced (corresponding to the resolution function of the apparatus) where $\varphi(u)=0$ for $|u|>a$ and

$$\int_{-a}^{+a}\varphi(u)du=1$$

where $a\ll(x_2-x_1)$, then

$$I=\int_{-\infty}^{\infty}\left\{\int_{-a}^{a}f(x+u)\varphi(u)du\right\}dx \qquad (9)$$

represents the corresponding integral when the resolution is not infinitely sharp. By integrating first with respect to x Eq. (8) reduces to

$$I=I_0\int_{-a}^{a}\varphi(u)du=I_0.$$

In comparing the area over the experimental transmission curve with that over $T_C(x)$, however, the range of integration is not infinite and does not vanish at the limits of integration x_1 and x_2. A more extended analysis shows that the difference $(I-I_0)$ depends only on the difference of the odd derivatives of $T_C(x)$ at x_1 and x_2 if $\varphi(u)$ is symmetric. Thus the principal effect is caused by the difference in the slopes $[f'(x_2)-f'(x_1)]$ and the correction is always small for the limits of integration chosen.

The area method of analysis is used only in obtaining the first approximation of the parameter B. In the final procedure the transmission curve calculated from the assumed value of B is integrated numerically over the resolution width of the apparatus and the value of the parameter which gives the best match between the calculated transmission curve and the experimental results is chosen. Therefore any error introduced in this part of the analysis will not affect the final results.

Other Factors Affecting the Transmission

The above analysis assumes that all the neutrons that do not reach the detector have been captured by the sample according to the Breit-Wigner one-level formula. However, it is also possible for neutrons to be removed from the beam by nuclear scattering or by some more complex molecular scattering and interference phenomena. Therefore, the decrease in the transmission due to these effects must also be taken into consideration.

When the resonance occurs at an energy appreciably above the thermal region, the cross section in the thermal region should consist of a $1/v$ capture term and another term which should be approximately constant over the energy region considered, and which will take into account all the other factors involved. Since the $1/v$ term gives a linear logarithmic plot on the time-of-flight basis, it is easy to resolve such a straight-line logarithmic plot into the sum of a constant term and a straight line through the origin. If the nuclear scattering cross section and the molecular and interference effects depend strongly on the energy of the incident neutron over the energy range measured, and if the variation in the scattering term is not negligible compared to the capture term, then the conclusions of this part of the analysis will be correspondingly reduced in significance. However, inspection of the results given in Fig. 10, for example, shows that the cross section in the thermal region can here be considered as consisting of a fixed term and a $1/v$ term and that in this case the other effects are sufficiently small in themselves or cancel each other in such a manner that the over-all effect is negligible.

METHOD OF MATCHING AN EXPERIMENTAL TRANSMISSION CURVE TO A MOST PROBABLE THEORETICAL CURVE BASED ON THE BREIT-WIGNER FORMULA

The material is first studied by investigating the transmission of a medium thick sample over the entire range of the apparatus with moderate resolution. This most quickly locates the regions of particular interest for closer investigation with higher resolution. These particular regions are then investigated more thoroughly with high resolution and with a different sample thickness if indicated.

The procedure used in analyzing the data for a definite sample will vary somewhat according to the particular properties of the sample itself but a few generalizations may be set up which usually represent the procedure employed.

1. A logarithmic plot of the transmission of the sample is made in the thermal energy region

for times-of-flight appreciably greater than t_0. The true transmission curve in this region is assumed to give a straight-line logarithmic plot and the best straight line through the experimental points is found by the method of least squares. This straight line is extrapolated to zero time-of-flight and the intercept at $t=0$ is taken to represent the transmission value, T_0, corresponding to the constant term in the total cross section.

2. The data in the vicinity of the resonance peak are plotted on a linear scale after the transmission at each point has been divided by T_0, the value of the intercept of the straight line obtained from the logarithmic plot of the transmission in Part 1.

3. The position of the minimum of the experimental transmission curve near the resonance is determined and a slightly lower time-of-flight value is chosen as t_0 because of the asymmetry of the transmission curve. The corrected transmission curve in the region of the resonance as obtained in Part 2 is then replotted in terms of the dimensionless parameter $x=(t-t_0)/t_0$.

4. The area above the transformed transmission curve from Part 3 between $x=-0.3$ and $x=0.5$ is then measured and an approximate value of B is obtained by the use of the graph given in Fig. 3.

5. Tables of values of T_c (theoretical transmission curves) are then computed using the exact relationship in Eq. (3) for several different values of B starting with the value of B found in Part 3 and with different values of λ^2 for each B. The transmission curve calculated for each separate value of B and λ^2 is then numerically integrated over the resolution function $\varphi(u)$ for several values of x to give T_t where

$$T_t=\int_{-a}^{a} T(x+u)\varphi(u)du, \qquad (10)$$

and $\varphi(u)$ is assumed to be triangular of width $2a$.

6. The shapes of several of these predicted curves are compared with the curves plotted in Part 2 and the set of values of B and λ^2 which gives the best fit is selected.

7. In the illustrations of these resonance absorption curves the curve obtained in Part 6 is then multiplied by the transmission due to the constant cross section and the calculated transmission curve is shown with the experimental results.

This procedure may of course be modified if the sample used is so thin that the decrease in transmission due to the constant cross section is negligible compared with the experimental error involved. In this case steps 1, 2, and 7 may be eliminated and steps 3, 4, 5, and 6 will be all that are necessary.

This method of analysis admittedly places great stress on both the theory and the experimental results, but it was felt that it would be of interest to see how good a match between a theoretical curve and the experimental results could be obtained. This method also has the advantage of reducing to a minimum all errors which would be introduced by more approximate methods of analysis. If two or more thicknesses of the same material are measured, the values of B and λ^2 obtained for one thickness of the absorber may be used to predict the transmission curve for the other absorber thicknesses to obtain an independent check on the uncertainties involved in the location of the parameters.

Paraffin Source and Source Detector Distance

The paraffin slab used as source of slow neutrons consisted of a 2.6-cm thickness of paraffin enclosed in a box of $\frac{1}{4}''$ thick plywood. The effective delayed emission time for thermal neutrons (times of flight of greater than 200 μsec/meter) was found to be about 45 μsec. The detector used was a BF_3 proportional counter in which the outer electrode was 20 cm long. The source detector distance was 5.4 meters measured from the detector side of the paraffin source slab to the center of the proportional counter. Thus an effective resolution broadening of 3.7 percent of the measured time-of-flight of the neutron was introduced because of the length of the counter. In the final analysis all results were reduced to the time-of-flight of the neutrons for one meter and the time-of-flight is usually expressed in μsec./meter.

These transmission measurements are always plotted on the time-of-flight basis because the resolution width of the apparatus is constant in this type of plot. If any other scale were used (velocity or energy) the result would give no

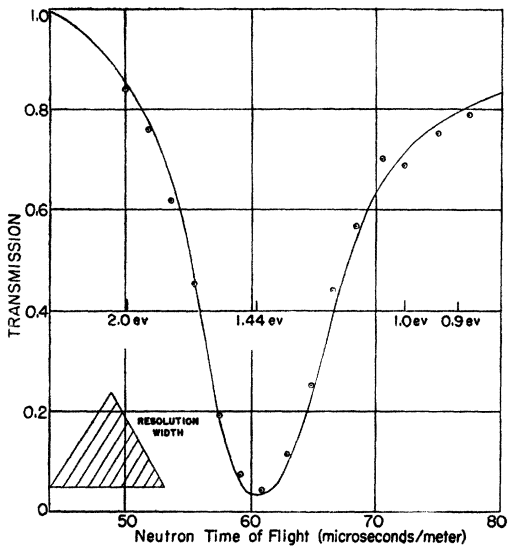

FIG. 4. The slow neutron transmission of 0.193 g/cm² of indium. The experimental points (circles) are compared with a calculated transmission curve (full line) based on the Breit-Wigner formula and the resolution function of the apparatus. The theoretical curve is for $E_0=1.44$ ev, $\sigma_0\Gamma^2=210\times10^{-24}$ (ev)² cm²/atom with $\Gamma=0.09$ ev.

indication of that portion of the transmission curve which the resolution width of the apparatus integrated over in order to determine the transmission of the sample at one point.

INDIUM

Two different samples were used for the indium transmission measurements. The thin sample contained 0.193 g/cm² of metallic indium and the thick sample contained 5.02 g/cm² of the metal. These samples were obtained from the Indium Company of America and were the purest indium that could be furnished by this company.

The results of the transmission measurements on the thin indium sample are given in Fig. 4 where the transmission is plotted as a function of the time-of-flight of the incident neutron for one meter. Each point represents the average of at least 8 separate pairs of measurements with the sample "in" and "out" of the beam. The over-all statistical accuracy of each point should be better than 5 percent. The resolution width of the apparatus is shown in the lower left corner of the figure. The total resolution width, which includes the cyclotron "on-time," detector on-time, counter pulse width, and the effect of the length of the counter, was taken to be 9 μsec./meter for the analysis given below.

Since the sample was thin, the scattering could not cause a difference in the transmission of more than 2 percent, therefore the data on this sample was analyzed according to the procedure given above assuming that the scattering had a negligible effect on the transmission.

The transmission minimum occurs at 60.2 μsec./meter so this value was chosen as t_0 for a first approximation. The area under the curve $(1-T)$ was calculated between 42 μsec./meter and 90 μsec./meter. The value $B=0.026$ was found from the theoretical curve given in Fig. 3. With this value of B the transmission at $t=t_0$ was calculated for several different values of λ^2. The value of λ^2 that gave the best agreement with the experimental transmission at the minimum of the curve was $\lambda^2=1\times10^{-3}$. The solid curve shown with the experimental points in Fig. 4 is the calculated transmission curve for $B=0.026$, $\lambda^2=1\times10^{-3}$, $t_0=60.2$ μsec./meter and an assumed resolution width of 9 μsec./meter. This corresponds to $\sigma\Gamma^2=210\times10^{-24}$ (ev)² cm²/atom and $\Gamma=0.09$ ev.

Although there seems to be satisfactory agreement between the theoretical curve and the experimental points in Fig. 4, the agreement is not completely indicated until the sensitivity of the agreement to variations in the parameters is shown. The shape of the theoretical transmission curve depends on the resolution width of the apparatus and the choice of the dependent parameters B and λ^2. The value of B can be determined to a fair degree of accuracy by the area method described above. As a check on this method, the transmission of the sample when $|t-t_0|\gg0$ is only very slightly affected by λ^2 and the resolution width of the apparatus. With the value of $B=0.026$, the calculated transmission at the edge of the resonance curve agrees fairly well with the experimental results.

The determination of the value of λ^2 is more difficult because it depends on the transmission of the sample at the minimum of the transmission curve where the correction due to the resolution width of the apparatus will also be a maximum. Therefore a small uncertainty in the value of the resolution width of the apparatus will cause

a large uncertainty in the value of λ^2 chosen to give a best fit.

In order to determine the magnitude of the effect of the resolution width of the apparatus on the choice of the value of λ^2 for best fit, the transmission at the minimum of the transmission curve was calculated as a function of the width of the level for several different resolution widths. The results of these calculations are given in Fig. 5. If the outside limit of error on the determination of the resolution width is taken as 1 μsec./meter, an estimate of the uncertainty in Γ, introduced by the uncertainty in the resolution width, can be made. From the curves given in Fig. 5 the value of Γ can only be said to lie between 0 ev and 0.16 ev. Thus this method of measuring the value of Γ will not give a very accurate value because of the uncertainty in the value of the resolution width.

Since the value chosen for B will also influence the choice of Γ for the best fit, the over-all uncertainty permits only an upper limit of 0.2 ev to be set on Γ.

In order to check the measurements made with the thin sample (0.193 g/cm^2) the transmission of the thick sample was measured in the thermal region. If only one level is assumed to be effective in the very low energy region, then the parameter B should determine the transmission in the thermal region. Since the parameter λ should have negligible effect at energies other than those in the immediate vicinity of the resonance peak, the parameter B can be located by use of Eq. (4), from the thick sample measurements.

When a thick sample is used, the changes produced in the transmission by a variation in B will be very large and consequently greater sensitivity can be obtained in the location of this parameter than in the measurements with a thin sample.

The calculated transmission curves in the thermal region using three different values of B for the thick sample, corresponding to the values $B=0.022$, 0.026, 0.034, for the thin sample are plotted logarithmically in Fig. 6 together with the experimental points for the transmission in this region. Since the ratio of the thicknesses for the two samples was 26, the values of B employed are also 26 times as large giving $B=0.572$, 0.676, 0.884.

The curve determined by the experimental points seems to follow the general shape of the theoretical curve very well thus indicating that only one level could be considered important in determining the thermal cross section. The experimental points seem to be slightly higher than the theoretical curve for $B=0.676$, thus indicating that the value chosen for B from the

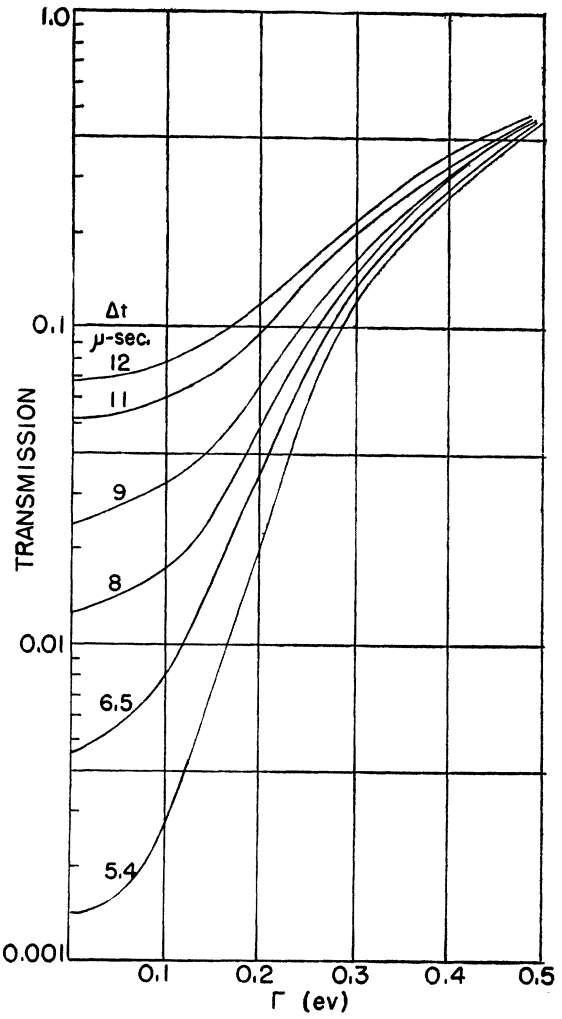

FIG. 5. The effect of Γ and the width of the resolution function on the transmission of the sample at the 60.2 μsec./m minimum of the indium transmission curve. The transmission at the minimum of the indium transmission curve has been calculated as a function of the width of the resonance level for several different resolution widths in order to show the effect that the resolution width of the apparatus has on the determination of the Γ from the experimental data.

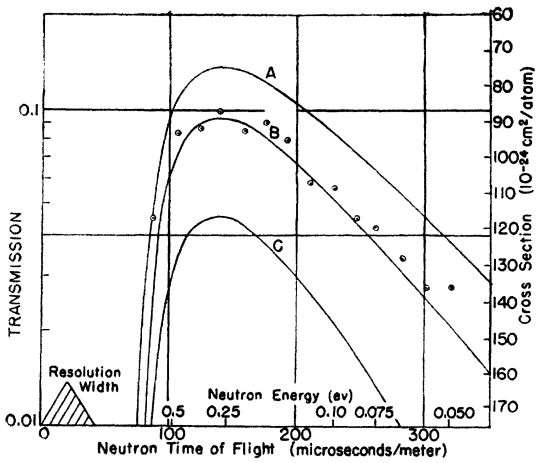

FIG. 6. The slow neutron transmission of 5.02 g/cm² of indium. The value of the effective sample thickness, B, is best determined for a thick sample from the maximum of the transmission curve between the resonance and the thermal region. The theoretical curves (full lines) are for the values of the parameters located from the measurements on the thin indium. Curve A: $B=0.572$ or $\sigma_0\Gamma^2=177\times10^{-24}$ cm² (ev)². Curve B: $B=0.676$ or $\sigma_0\Gamma^2=210\times10^{-24}$ cm² (ev)². Curve C: $B=0.884$ or $\sigma_0\Gamma^2=274\times10^{-24}$ cm² (ev)².

experimental results on the thin sample was slightly large. This would be further accentuated by the fact that the constant cross section has not been taken into consideration.

The method for determining the constant cross section described above cannot be applied accurately in the case of indium because the resonance level occurs at too low an energy. Therefore, the assumption that the capture cross section is directly proportional to the time-of-flight would not be valid until the energy was below about 0.07 ev. Measurements were not carried much below this energy because of the extremely low transmission of the sample which was available.

If the value for the constant cross section of indium is arbitrarily chosen as being the same order of magnitude as for silver and antimony, and less than that for nickel, a value for σ (const.) between 4×10^{-24} and 10×10^{-24} cm²/atom would be appropriate. Choosing the upper value will shift the theoretical curves in Fig. 6 down by the factor 0.77. In this case the value of B chosen would not be lower than 0.572 as this curve, when lowered the required amount, still lies observably above the experimental points.

Taking into account all the factors involved, the final results can be given as

$E_0=(1.44\pm0.04)$ ev,
$\sigma_0\Gamma^2=(210\pm60)\times10^{-24}$ cm² (ev)²,
$\Gamma<0.2$ ev ($\Gamma=0.09$ ev),
$\sigma_0>5200\times10^{-24}$ cm²/atom
($\sigma=26{,}000\times10^{-24}$ cm²/atom).

GOLD

In studying the transmission of gold as a function of the time-of-flight of the incident neutrons two different thicknesses of gold foils were used. The first contained 0.2100 g/cm² and the second contained 0.856 g/cm². Both of these samples were fine gold obtained from Handy and Harman of New York City, who state that the purity is better than 99.999 percent. Since both of these samples can be classed as thin, no discussion of the measurements on the thinner of the two samples seems necessary as more accurate data can be secured using the thicker sample. The results of the measurements on the thinner sample are introduced to show the self-consistency of the results for two different sample thicknesses.

The results of the transmission measurements for the two gold samples are given in Fig. 7. The upper curve, of course, is for the thinner

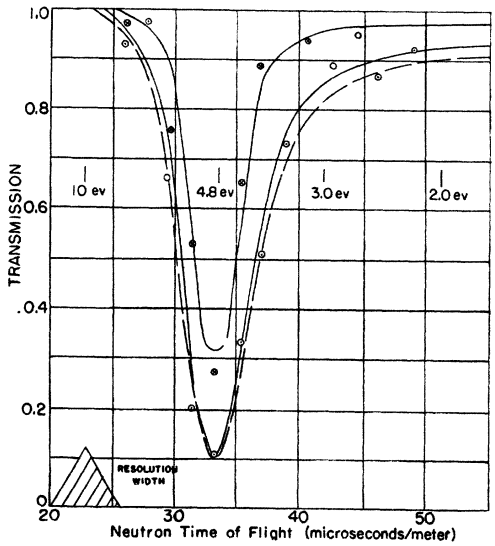

FIG. 7. The slow neutron transmission of 0.210 g/cm² and 0.856 g/cm² of gold. The solid curves are based on the Breit-Wigner formula and the resolution function of the apparatus with $\sigma_0\Gamma^2=600\times10^{-24}$ cm² ev²/atom and $\Gamma=0$. The dashed curve is for $\sigma_0\Gamma^2=655\times10^{-24}$ cm² ev²/atom and $\Gamma=0.5$ ev. ⊙—Experimental points for 0.856 g/cm² sample: ⊗—Experimental points for 0.210 g/cm² sample.

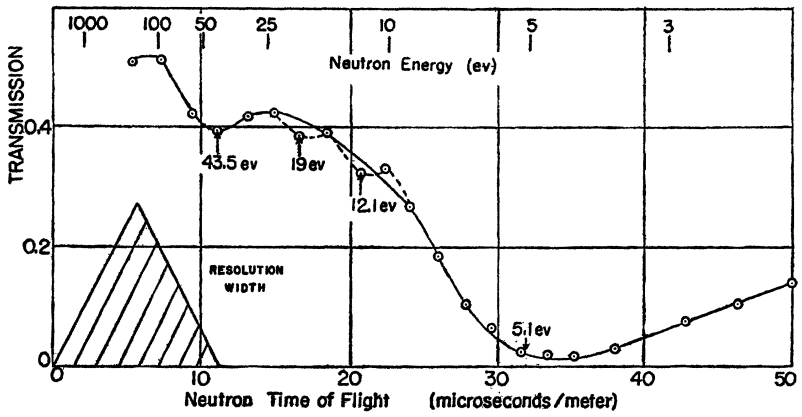

FIG. 8. The slow neutron transmission 19.8 g/cm² of silver. This is a typical preliminary transmission curve using a thick sample to explore a wide energy range as a basis for further investigations using appropriate sample thicknesses. With this sample thickness, the principle resonance at 5.1 ev is flattened to extend over a considerably wider range than is desirable for accurate analysis.

sample. The resolution width of the apparatus is shown in the lower left-hand corner of the figure. The position of the minimum in both curves seems to occur at about 33.5 microseconds/meter. Since the resolution width of the apparatus is fairly wide compared to the width of the resonance line, the value of $t_0=33$ microseconds/meter was chosen as a first approximation for the resonant time-of-flight.

The analysis described above was applied to the data for the thicker sample and the values of the parameter which gave the best fit to the experimental points were $B=0.017$, $\lambda^2=0$. Because of the relatively poor resolution used here, it is not surprising that the value for the width of the line should come out zero. This only means that no lower limit can be set for the width of the line although it is possible to set an upper limit as previously described. This upper limit was taken as $\lambda^2=3\times10^{-3}$. With this value of λ^2 and the value of $B=0.022$ which gave the transmission at the minimum point the dashed theoretical transmission curve in Fig. 7 was definitely too low at the edge of the resonance dip. The two solid curves in the graph represent the theoretical curve for the two different samples with $B=0.017$, $\lambda^2=0$ for the thicker sample and $B=0.0042$, $\lambda^2=0$, as corresponding values for the thinner sample. The values for the thinner sample are equal to the ones for the thicker sample when multiplied by the thickness ratio so a direct comparison of the consistency of the results for the two thicknesses may be made.

The values for the physical constants corresponding to these values of the parameters and their uncertainties are:

$$E_0=(4.8\pm0.2)\text{ ev},$$
$$\sigma_0\Gamma^2=(600\pm80)\times10^{-24}\text{ (ev)}^2\text{ cm}^2,$$
$$0<\Gamma<0.5\text{ ev},$$
$$\sigma_0>2400\times10^{-24}\text{ cm}^2.$$

The Breit-Wigner theory of neutron capture sets an upper limit on the cross section at resonance as $\sigma_0\leq\pi\lambda^2$, where $2\pi\lambda$ is the wavelength of the resonant neutron (2).

Since gold has only one isotope

$$\sigma_0\leq178{,}000\times10^{-24}\text{ cm}^2$$

therefore $\Gamma>0.06$ ev.

Feeney, Lapointe, and Rasetti[12] reported from indirect measurements that there were some indications of more than one resonance level in the gold spectrum, but no indication of another level within the range of the instrument was found in these investigations. The energy of the gold resonance found by them was quite different from the value reported here. However, the discrepancy seems to lie in the value of the effective thermal energy which was assumed in the boron absorption method employed by that group.

If their value for the boron absorption at the energy of the resonance is used together with the

energy dependence of the boron cross section as determined in the previous paper[1] then the difference between their value and the one found here is not appreciable.

SILVER

The selection of a sample for the study of the resonance absorption of neutrons by silver offers a more complex problem than for indium or gold because silver was known to have more than one level present for neutron energies of the order of a few electron volts. Therefore, the trial and error method was applied in the selection of the sample. All the silver samples were purchased from Handy and Harman and were the purest silver obtainable. There was no copper impurity detectable.

Since previous experience had indicated that a thick absorber was good for the preliminary study, a 19.8 g/cm² disk of metallic silver was used. The transmission of this sample as a function of the time of flight of the incident neutron is shown in Fig. 8 with the resolution width of the apparatus indicated in the lower left-hand corner of the figure. It is immediately obvious from this curve that one level is predominant as far as this type of measurement is concerned. The predominant level has its maximum absorption at 32 microseconds/meter. Another level can easily be detected at 11 microseconds/meter, and others might be present at about 17 and 21 microseconds/meter but no definite conclusions are warranted from this data. The transmission of this sample is so low near the 32 microsecond/meter resonance and the effects of this level are so strong that little more can be said from these results.

Because the one level at 32 microseconds/meter is so predominant on the time-of-flight basis, the transmission of a *thin* absorber will be affected by this level only, in the vicinity of this level, and the effects of the other levels will be negligible. Therefore transmission measurements were made using a thin sample containing 1.043 g/cm², in the vicinity of 32 microseconds/meter. The highest resolution consistent with useful intensity was employed in these measurements, the results of which are given in Fig. 9. The shape of the curve looks very much like the curve obtained for the gold transmission measurements, indi-

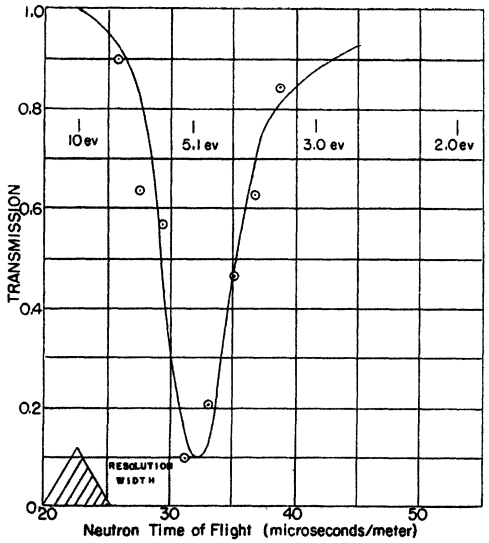

FIG. 9. The transmission of 1.046 g/cm² of silver. This is a "thin" sample, used to study the main resonance at 5.1 ev. The solid curve is a calculated transmission curve for one level at $E_0=5.1$ ev with $\sigma_0\Gamma^2=300\times10^{-24}$ cm² ev²/atom and $\Gamma=0$.

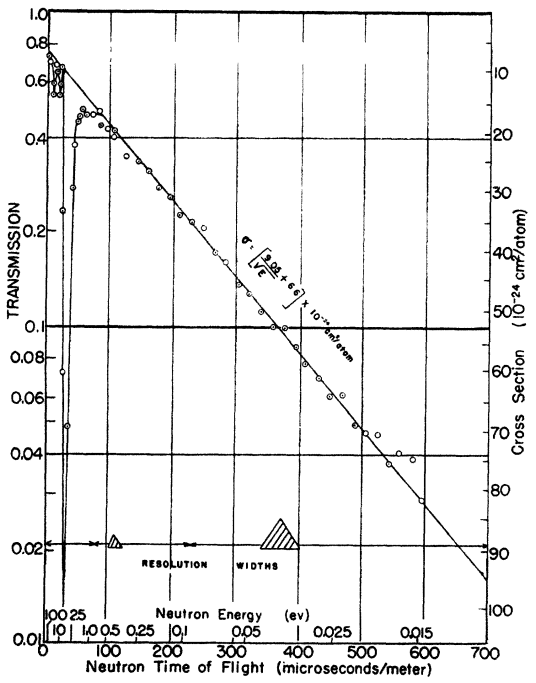

FIG. 10. The slow neutron transmission of 7.84 g/cm² of silver. A sample of intermediate thickness was best for a study of the entire region of investigation. The transmission curve, except for the resonance region, can easily be resolved into the sum of a constant cross section and a $1/v$ term. The relative sharpness of the levels for this type of measurements is also well illustrated.

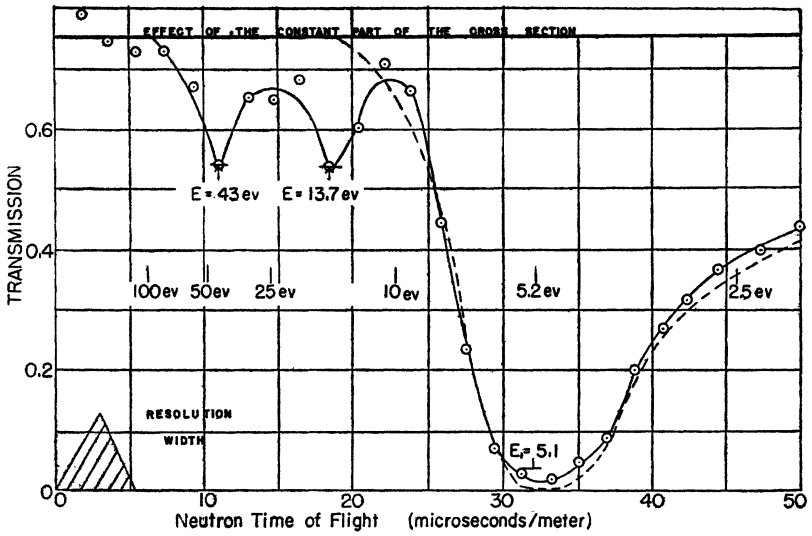

FIG. 11. The slow neutron transmission of 7.84 g/cm² of silver in the resonance region. The high energy portion of the previous plot is expanded to show resonances at 43 ev, 13.7 ev, and 5.1 ev. The dashed curve is a calculated curve for one level based on the parameters located from the transmission of the 1.046 g/cm² sample. The "strengths" of the two higher energy levels obtained from the magnitude of the transmission dips in this figure are $\sigma_0\Gamma^2 = 380\times10^{-24}$ cm² ev²/atom for the level at 43 ev and $\sigma_0\Gamma^2 = 14\times10^{-24}$ cm² ev²/atom for the level at 13.7 ev. The constant cross section factor was located from Fig. 10.

cating that little error is introduced by assuming only the one level to be effective in this region. The standard method of analysis was applied to this data, assuming that only the one level was effective in producing this absorption and that the constant cross section was unimportant. The theoretical curve given in Fig. 9 along with the experimental points is for $B=0.017$, $\lambda^2=0$. As was also true in the case of gold, the effects of small changes in λ^2 are negligible when the relative resolution is as low as in this case. No attempt has been made to set an upper limit on λ^2 because of the assumptions made as to the magnitude of the effects of the other levels and of the constant cross section. Therefore $\sigma_0\Gamma^2 = 300\times10^{-24}$ (ev)² cm² was taken as the effective "strength" of this level and $t_0=32$ microseconds/meter was taken as the resonant time-of-flight. This corresponds to a resonant energy $E_0=(5.1\pm0.2)$ ev.

A preliminary run on the thin sample in the thermal region gave sufficient data to indicate the thickness of the sample which would give best results in this region. Therefore, the thick sample was cut approximately in half and a sample containing 7.84 g/cm² was used for the rest of the measurements on silver.

The results of the transmission measurements with this sample are given in Figs. 10 and 11. In Fig. 10 the transmission is plotted logarithmically as a function of the time-of-flight of the incident neutron over the full range of the measurements taken. The resolution width of the apparatus was varied for different portions of the curve, as indicated by the triangles given at the base of the figure. In Fig. 11 the region between 0 and 50 microseconds per meter has been expanded on a linear plot to show the region in which the resonance levels are detected.

The full method of analysis described above was applied to the data on this sample. The straight line which *best fits* the experimental points on the logarithmic plot has its intercept at $T=0.75$. This corresponds to a constant term in the cross section of silver of approximately 6.6×10^{-24} cm²/atom. The equation of this straight line as a function of the energy of the incident neutron is

$$\sigma_0=(9.05E^{-\frac{1}{2}}+6.6)\times10^{-24}\ \text{cm}^2/\text{atom},$$

where E is in electron volts.

Assuming the constant part of the cross section for silver to be 6.6×10^{-24} cm² as determined from

the data given in Fig. 10 and assuming that $\sigma_0\Gamma^2 = 300\times10^{-24}$ (ev)^2 cm^2 for the level at 5.1 ev as determined from the data given in Fig. 9, the form of the transmission curve was calculated in the vicinity of 32 microseconds/meter. This curve is the dashed curve in Fig. 11. The calculated curve seems to agree fairly well with the experimentally determined points.

In the measurements using the 7.84 g/cm^2 sample with the highest resolution obtainable the two less noticeable levels in this type of measurements which had been tentatively located using the 19.8 g/cm^2 sample were confirmed. Although from the appearance of the curve it may seem that too much stress has been placed on the points at 11.1 and 19.4 microseconds per meter, the values of the transmission shown in Fig. 11 by the points are each the average of at least eight separate pairs of measurements and have a statistical accuracy of better than 3 percent. Also these levels were tentatively located with the thicker sample so that their reality seems plausible. An approximate value of B was determined for each of these levels. The accuracy of this value is probably accurate to about a factor of 2 because of the relatively poor resolution of the instrument in this region and the confusion due to several levels.

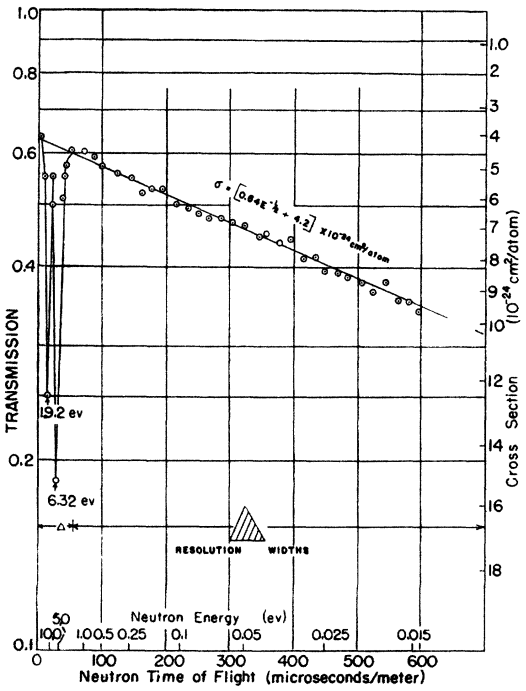

FIG. 12. The slow neutron transmission of 22.41 g/cm^2 of antimony. This shows the transmission of antimony throughout the entire region of investigation and shows the method of locating the constant cross section and the $1/v$ curve in the thermal region. The relative position of the resonances is also indicated.

Taking into consideration all of the facts involved in the measurements on silver the final results may be given as

$$E_1 = (5.1\pm0.2) \text{ ev},$$
$$\sigma_1\Gamma_1^2 = (300)\times10^{-24} \text{ (ev)}^2 \text{ cm}^2/\text{atom}.$$
$$E_2 = (13.7\pm1) \text{ ev},$$
$$\sigma_2\Gamma_2^2 = (14)\times10^{-24} \text{ cm}^2 \text{ (ev)}^2/\text{atom}.$$
$$E_3 = (43\pm5) \text{ ev},$$
$$\sigma_3\Gamma_3^2 = (380)\times10^{-24} \text{ cm}^2 \text{ (ev)}^2/\text{atom}.$$
$$\sigma_{\text{thermal}} = \{(9.05\pm0.30)E^{-\frac{1}{2}} + (6.6\pm0.5)\}\times10^{-24} \text{ cm}^2/\text{atom}$$

where E is in ev.

ANTIMONY

For the measurements on antimony the heaviest sample available was used in order to give sufficient neutron absorption in the thermal region and at the resonances for accurate measurements to be made. The sample used contained 22.41 g/cm^2 of metallic antimony. Even then the lowest transmission at the minimum of a resonance dip was only 18 percent. This sample was cast by the Mackay Laboratories from antimony metal of the analytical reagent grade.

The results of the transmission measurements on antimony are shown in Figs. 12 and 13. The resolution width of the apparatus was considerably different for the resonance energy region than for the thermal region as is indicated at the bottom of Fig. 12. The results given in Fig. 13 show very definite dips in the transmission at 16.5 microseconds/meter and at 28.7 microseconds/meter. There also seems to be a broad dip in the transmission between 0 and 10 microseconds/meter with its center at about 6 microseconds/meter. This dip in the transmission at the lower time-of-flight might be caused by one very broad level at 6 microseconds/meter but, for reasons mentioned below, it is probably caused by many levels spread out over this energy region which are too narrow and too closely spaced to be resolved in these measurements. The minima at 16.5 microseconds/meter and at 28.7 microseconds/meter correspond to energies of 19.2 ev

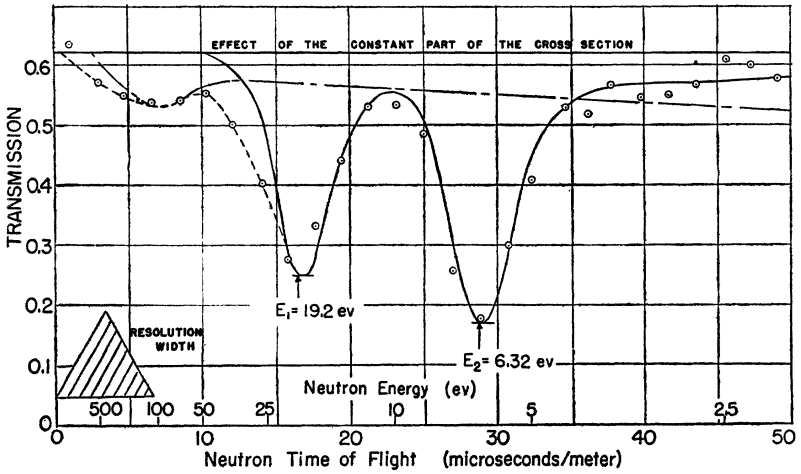

FIG. 13. The transmission of 22.41 g/cm² of antimony in the resonance region. The two main resonances and indications of others at higher energies are seen from the dips in the transmission below the value due to the constant term located from Fig. 12. The solid curve is a calculated transmission curve for two independent levels at 19.2 and 6.3 ev with $\sigma_0\Gamma^2=210\times10^{-24}$ cm² ev²/atom for the level at 19.2 ev and with $\sigma_0\Gamma^2=20\times10^{-24}$ cm² ev²/atom for the level at 6.3 ev. The dot-dashed curve is an attempted fit for the high energy dip assuming a single level with $E_0=145$ ev and $\Gamma=92$ ev. The effect of this level would be much too large in the thermal region and too small in the resonant region indicating the probability of many interfering levels.

and 6.3 ev, respectively. A timing of 6.0 microseconds/meter corresponds to an energy of 145 ev.

The standard method of analysis was applied to the results of the transmission measurements in the thermal region and the intercept of the straight line was located as $T=0.64$. The equation of the straight line which best fits the experimental results in the thermal region given in Fig. 12 is

$$\sigma_{\text{thermal}}=\{(0.64\pm0.02)E^{-\frac{1}{2}}+(4.2\pm0.4)\}\times10^{-24}\ \text{cm}^2/\text{atom}$$

where E is in electron volts.

The constant term in the cross section for antimony was therefore taken as 4.2×10^{-24} cm²/atom and the best values of B were located for the 16.5 and 28.7 microsecond/meter resonances assuming each to be a single independent level. The separate calculated transmission curves for the two levels were then multiplied together to give an over-all theoretical transmission curve for the two levels. This curve was then numerically integrated over the resolution function of the apparatus to give the solid curve shown in Fig. 13. In all cases the value of λ was assumed to be zero and no attempt was made to set an upper and lower limit on Γ. Since the resolution width of the apparatus is relatively broad in this energy region, the sensitivity of the shape of the transmission curve to variations in B is not large. When the additional effect of small uncertainties in the determination of the constant part of the cross section is considered, the over-all accuracy of the value selected for the parameter B is probably accurate to about a factor of 2.

An attempt was made to fit a calculated transmission curve to the experimental results in the vicinity of 6 microseconds/meter assuming that only one broad level is present. The dot-dash curve in Fig. 13 shows the calculated transmission due to a level at 145 ev with a width of 92 ev. The area between this curve and the line $T=0.64$, which corresponds to unity transmission for capture, is seen to be much less than this same area for the experimental curve in the region between 4.2 and 9.0 microseconds/meter. Therefore the value of B required for one level to give the observed area would have to be even larger than that chosen. The area of the absorption dip in the resonance region has a different dependence on the parameter B than the corresponding absorption in the thermal region. The area of the absorption dip in the resonance region depends

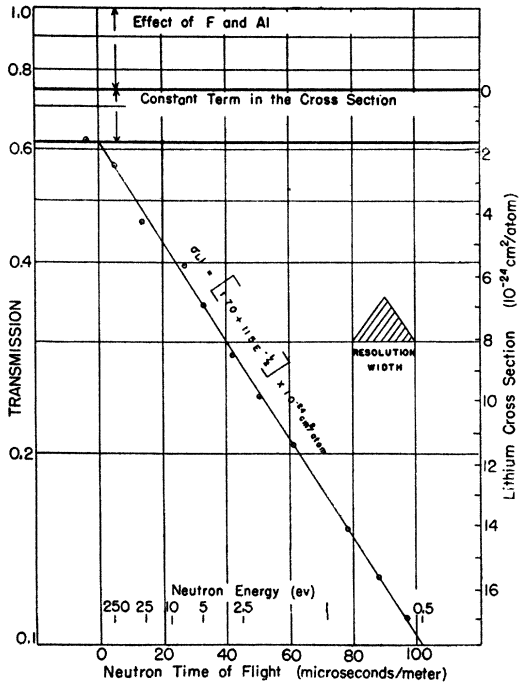

FIG. 14. The slow neutron transmission of 4.85 g/cm² of lithium fluoride. The logarithmic plot of the transmission of lithium can easily be resolved into a straight line with $\sigma=(1.7+11.5E^{-\frac{1}{2}})\times10^{-24}$ cm²/atom if the cross section of fluorine is assumed to be constant at 2.5×10^{-24} cm²/atom. The high energy region is emphasized in this plot.

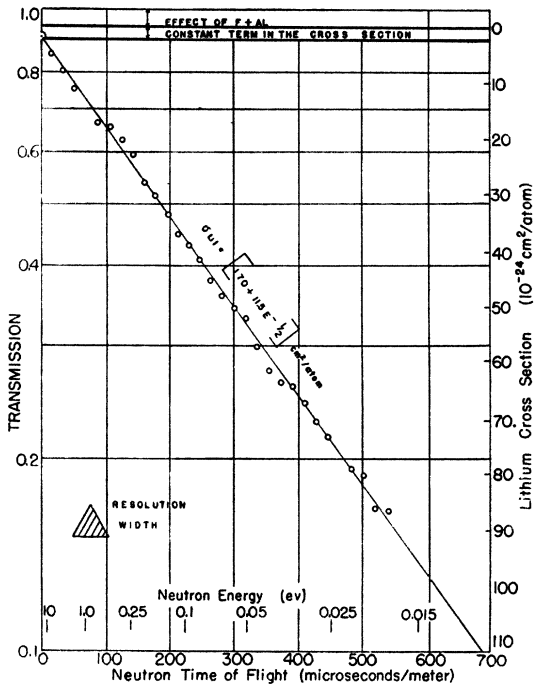

FIG. 15. The slow neutron transmission of 0.862 g/cm² of lithium fluoride. The *same* $1/v$ and constant term in the cross section have been taken for the straight line drawn in this plot as were taken for the much thicker sample used in Fig. 14. A much wider range is covered showing good agreement with the results on the thicker sample.

on $\sqrt{B}$ while the corresponding absorption in the thermal region depends on B itself. When the effects of several levels are combined in the resonance region the total area under the absorption curve will be proportional to the sum of the $\sqrt{B}$ terms for each level with slight chance of interference if the levels do not overlap appreciably. In the thermal region the area under the absorption curve increases as the sum of the separate B values therefore the increase in absorption in the thermal region will be relatively much slower than the corresponding increase in absorption in the resonance region. In addition the interference effects between several levels could be very pronounced in the thermal energy region which is quite a distance from the resonance energy region of all the levels. Suppose, for example, there are four levels of equal strength which together produce a specified area for absorption in the resonance region. Then the corresponding absorption in the thermal region will be at most one-half as much as that which would occur if only one level had been responsible for the total resonance absorption. Interference effects between the levels might then further reduce the relative thermal absorption to much less than the value one half.

The predicted absorption in the thermal region due to only the two easily resolved levels at 16.5 and 28.7 microseconds/meter is approximately the same as the experimentally observed absorption. The predicted absorption in the thermal region due to only the one level at 6.0 microseconds/meter is several times larger than that actually observed. Therefore, considering all the factors involved, it seems quite likely that the transmission dip in the vicinity of 6 microseconds/meter is caused by several unresolved levels which probably interfere considerably in the thermal region.

The results of the transmission measurements on antimony may be summarized as

$$E_1=(19.2\pm1.0)\text{ electron volts }\sigma_1\Gamma_1^2$$
$$=(210)\times10^{-24}\text{ (ev)}^2\text{ cm}^2,$$

$E_2 = (6.3 \pm 0.2)$ electron volts $\sigma_2 \Gamma_2^2$
$= (20) \times 10^{-24}$ (ev)^2 cm^2,

$\sigma_{\text{thermal}} = [(0.64 \pm 0.02)(E)^{-\frac{1}{2}} + (4.2 \pm 0.3)]$
$\times 10^{-24}$ cm^2/atom.

Other levels above 50 ev not resolved.

LITHIUM

Lithium fluoride was the substance used as an absorber for the transmission measurements on lithium. This salt was tightly packed in an aluminum container such that there were 4.85 g/cm^2 of LiF and 0.418 g/cm^2 of aluminum in the beam for the thicker sample and 0.862 g/cm^2 of LiF and 0.418 g/cm^2 of aluminum in the beam for the thinner sample. The lithium fluoride was obtained from the City Chemical Corporation and was of analytical reagent grade. The salt was dried at 120°C for 48 hours before being packed in the container.

The results of the transmission measurements on these two samples are given in Figs. 14 and 15. The experimental points can easily be fit to a straight line on a logarithmic plot. This straight line has its intercept at $T = 0.905$ for the 0.862 g/cm^2 sample and at $T = 0.614$ for the 4.18 g/cm^2 sample. If the cross section of aluminum is assumed to be 1.5×10^{-24} cm^2/atom and that of fluorine 2.5×10^{-24} cm^2/atom[4,5] and these cross sections are assumed constant over the energy interval studied, then the absorption due to the aluminum and the fluorine will be equivalent to a reduction in the transmission to $T = 0.938$ for the 0.862 g/cm^2 sample and to $T = 0.826$ for the 4.85 g/cm^2 sample. The experimental results then indicate that the slow neutron cross section of lithium follows a $1/v$ law and may be expressed as:

$\sigma_{\text{Li}} = [(11.5 \pm 0.2)(E)^{-\frac{1}{2}} + (1.7 \pm 0.2)]$
$\times 10^{-24}$ cm^2/atom,

where E is expressed in electron volts.

The cross sections of aluminum and fluorine in the thermal region are known to be small and almost entirely due to scattering. The variation of their cross sections over the energy region considered should be small and thus introduce negligible error in the determination of the slope of the line which best fits the experimental results.

However, the determination of the constant term in the expression for the cross section of lithium is directly dependent on, and of the same order of magnitude as, the cross section for the aluminum and fluorine. Therefore, this value depends directly on the assumed values of the cross sections of aluminum and fluorine. The effect of the absorption of the aluminum is the same for both samples and is equivalent to a reduction in the transmission to $T = 0.986$; therefore a 10 percent error in the assumed aluminum cross section will introduce an error of less than 0.7 percent in the determination of the constant term in the expression for the cross section from the results on the 4.85 g/cm^2 sample. However, the absorption due to the fluorine increases with the sample thickness in the same proportion as that of the lithium. The cross section of fluorine is known quite well[5] and a 5 percent error in the assumed cross section will change the value of the constant cross section by about 7 percent which is well within the precision stated.

The constant term in the expression for the

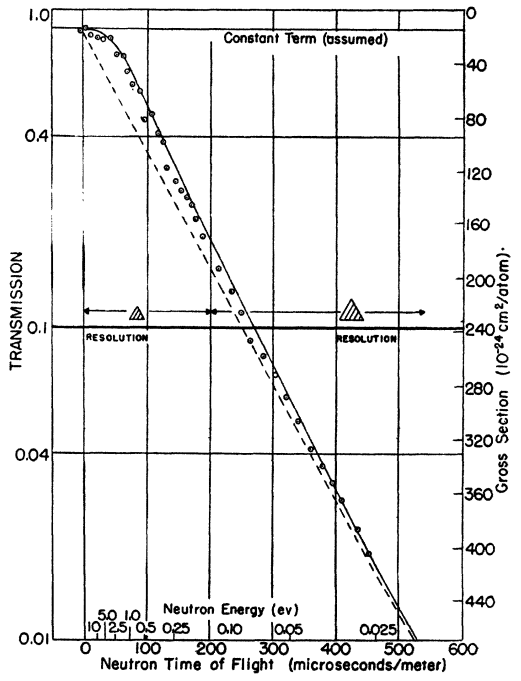

FIG. 16. The slow neutron transmission of 3.25 g/cm^2 of mercury. The solid curve in the figure is a theoretical transmission curve for a negative level at -2.0 ev. The dotted line represents the corresponding $1/v$ line determined from these data. The constant term in the cross section was taken from Figs. 17 and 18.

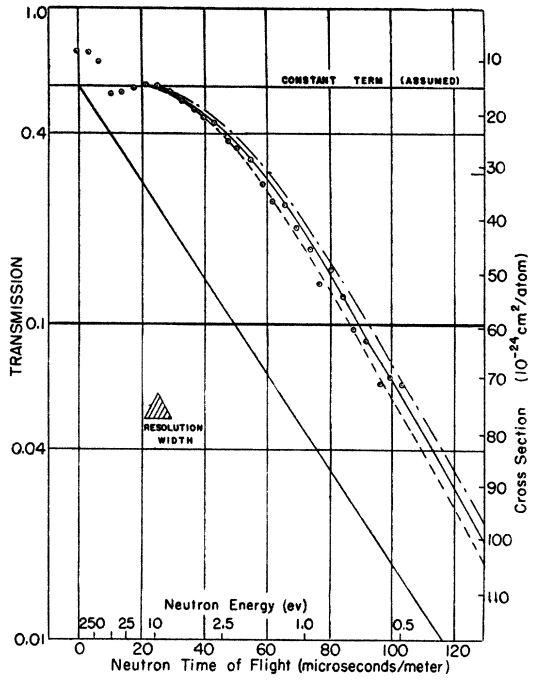

FIG. 17. The slow neutron transmission of 12.9 g/cm² of mercury. The curves shown in this figure are theoretical transmission curves based on the $1/v$ factor determined from Fig. 16. Dashed curve: $E_0=-2.25$ ev. Full curve: $E_0=-2.00$ ev. Dot-dash curve: $E_0=-1.75$ ev. Heavy straight line: $\sigma=[15+64E^{-\frac{1}{2}}]\times10^{-24}$ cm²/atom. The constant term in cross section was located by a process of trial and error.

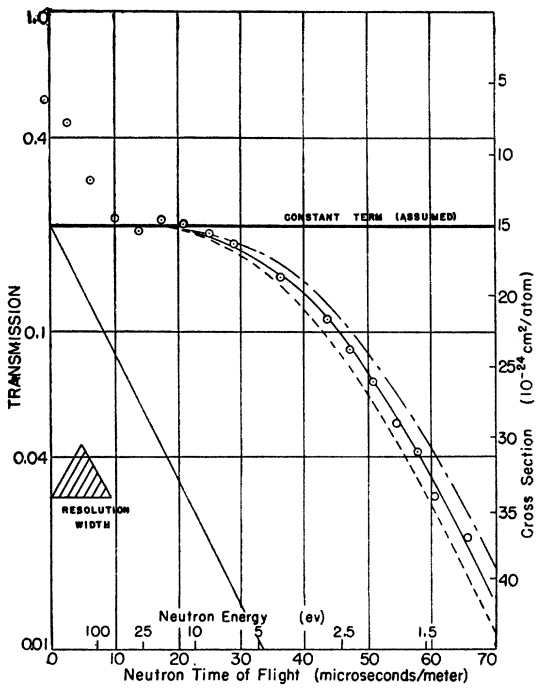

FIG. 18. The slow neutron transmission of 34.4 g/cm² of mercury. The curves shown here are for the same set of theoretical parameters as used in Fig. 17. The close agreement of the curve for $-E_0=-2.0$ ev for the three greatly different sample thicknesses of Figs. 16–18 show that there can be no appreciable systematic errors in the method. The common disagreement with the theoretical curve above 10 ev indicates the existence of positive levels.

cross section of lithium is equal to the capture cross section at approximately 45 ev. If the constant part of the cross section is assumed to be caused only by scattering then this value agrees qualitatively with the order of magnitude calculations given by Bethe.[2]

MERCURY

For the transmission measurements on mercury several brass containers were constructed to hold different thicknesses of liquid mercury. The side walls of all the containers were made of the same thickness brass plate and the slow neutron transmission of all the holders were compared and found to be the same. The use of an empty container on the "out" runs thus eliminates the effect of the container on the results. The mercury was U.S.P. XII redistilled—purchased from the Mallinkrodt Chemical Works.

For the preliminary investigation of the entire transmission curve of mercury, a sample containing 3.25 g/cm² of the liquid was used. The results of these transmission measurements are shown in Fig. 16. It is at once evident from these results that the nature of this transmission curve is qualitatively different from the transmission curves of the other elements studied. For a material with a positive resonance the logarithmic plot of the transmission is a straight line over most of the energy range studied and the actual transmission dips below this straight line in the region of the resonance. In Fig. 16 the logarithmic plot of the transmission also gives an approximately straight line in the region of large timings (low energies) but then it differs from the other curves in that the transmission is much higher than the $1/v$ line in the region of the higher energies. This is the type of transmission curve that would be expected from an element having a resonance level below the binding energy of the neutron. The solid curve that is shown with the

experimental results in Fig. 16 is for a negative energy of -2.0 ev.

For a negative energy level the Breit-Wigner one-level formula for neutron capture is of the form

$$\sigma=\sigma_0\left[\frac{E_0}{E}\right]^{\frac{1}{2}}\frac{\Gamma^2}{\Gamma^2+4(E+E_0)^2},$$

where $-E_0$ is the resonant energy. If $E_0\gg\Gamma$, then the first term in the denominator will always be small compared to the second and consequently can be neglected. The equation may then be written

$$\sigma=\left[\frac{\sigma_0\Gamma^2}{4E_0^{\frac{1}{2}}}\cdot\frac{1}{E^{\frac{1}{2}}}\right]\left[1+\frac{E}{E_0}\right]^{-2}.$$

In this expression the first bracket represents the $1/v$ straight-line term in the cross section. The second bracket is the expression that is of interest in locating the negative resonance energy. If $E\ll E_0$, then the value of the second bracket is approximately unity and the cross section follows a $1/v$ curve. As E/E_0 approaches unity or larger, the cross section becomes appreciably smaller than the $1/v$ relation and gradually changes into a $1/v^5$ dependence.

In matching the experimental results to a theoretical curve of this type three parameters must be evaluated. The first of these is the constant term which must be deducted from the cross section before any other analysis can be applied. The second is the slope of the $1/v$ curve in the thermal region and the last is the energy of the negative resonance level. A trial and error method was applied to the results of the transmission measurements on the 3.25 g/cm^2 sample. Several theoretical curves with different $1/v$ factors and different negative energy values were calculated and the shapes of these curves were compared with the shape of the experimental curve. By this process it was found that the agreement in the thermal region was very sensitive to a change in the $1/v$ factor but relatively insensitive to a change in the value chosen for the resonant energy. The agreement in the higher energy region (in the vicinity of 30–100 microseconds per meter) is most sensitive to a change in the value chosen for the resonant energy and less sensitive to a change in the $1/v$ factor. Since this region can be studied with much greater accuracy using a thicker sample only the $1/v$ factor was obtained from the results on the 3.25 g/cm^2 sample. The assumed constant cross section shown in Fig. 16 was located from the thicker sample. The resulting theoretical curve for a negative resonance energy of 2.0 ev is shown in Fig. 16 for comparison with the experimental points. It can easily be seen from these results that the $1/v$ factor cannot be changed by as much as 5 percent without causing the theoretical curve to be appreciably different from the experimental results.

In Figs. 17 and 18 the results of the transmission measurements on a 12.9 g/cm^2 sample and a 34.4 g/cm^2 sample are shown for the entire region of investigation of these samples. In Fig. 19 the high energy region for the thicker sample has been expanded to give some indication of the behavior of the transmission in this region. These results clearly show a broad shallow dip in the transmission between 10 and 15 microseconds/meter with a maximum in the transmission near 20 microseconds per meter. The cross section seems to be of the order of 7×10^{-24} cm^2/atom in the vicinity of zero time-of-flight. For the purpose of analysis of the

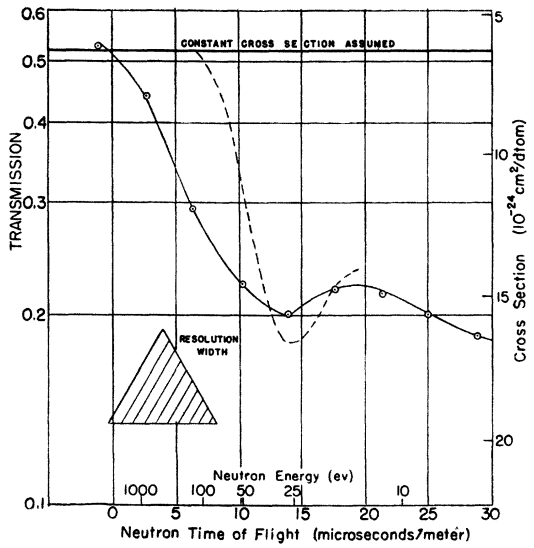

FIG. 19. The slow neutron transmission of 34.4 g/cm^2 of mercury in the high energy region. The solid curve follows the experimental points indicating resonances above 25 ev. The dotted curve is a theoretical curve for a single level at $E_0=31.4$ ev with $\Gamma=37.8$ ev showing the probable existence of several levels above 25 ev to give the observed broad dip.

negative energy level the shape of the curve for timings below 20 microseconds/meter was assumed to be caused by several levels which interfered with each other in such a manner that their over-all contribution to the cross section for energies below 10 ev could be neglected compared to the effect of the negative level. The possible effects of these positive levels will be discussed further below.

Using the $1/v$ factor located from the results on the 3.25 g/cm^2 sample several transmission curves were calculated for the two thicker samples, using different values of the resonant energy. The shapes of these curves were compared with the shapes of the experimental transmission curves as shown in Figs. 17 and 18. Since the constant cross section corresponds to a constant distance on a logarithmic transmission plot, the value of the constant cross section which will give the best fit to a theoretical curve can be found by inspection. A preliminary value of $\sigma_{\text{const}}=15\times10^{-24}$ cm^2/atom was therefore chosen.

When the constant cross section is determined and the $1/v$ term is also located, it is possible to calculate a value of E_0 from each of the experimental points. These calculations were carried out for the results on the 34.4 g/cm^2 sample. Because of the nature of the dependence of the transmission on the timing only the values of the transmission at timings greater than 30 microseconds/meter were considered. Using a value of $\sigma_c=15\times10^{-24}$ cm^2/atom for the constant cross section the calculated values of E_0 were fairly constant giving a value of $E_0=-(1.95\pm0.02)$ ev where the probable error given considers only the internal consistency of the results. This does not indicate the accuracy of the determination but it does show the degree of internal agreement of the calculated values. In order to test the sensitivity of the determination of the negative resonance energy to changes in the chosen value of the constant cross section the values for the resonant energy were again calculated using first a greater and then a smaller value for the constant cross section. If a value of $\sigma_c>15\times10^{-24}$ cm^2/atom is used, the calculated numerical value of $|E_0|$ will be small for low times of flight and increase to approach the value of $-E_0=2.0$ ev for larger times of flight. Similarly if the values of $\sigma_c<15\times10^{-24}$ cm^2/atom is used, the calculated value of $|E_0|$ will be too large for low times of flight and will decrease to approach the value of $-E=2.0$ ev for larger times of flight. Thus the requirement that the constant term be chosen in such a manner that the calculated value of E_0 does not systematically change with the timing dictates that the constant term to be deducted for the analysis of the negative level be $\sigma_c=15\times10^{-24}$ cm^2/atom and the resulting energy of the negative resonance be $-E_0=2.0$ ev.

For reference the calculated transmission curves for $-E_0=1.75$ ev, 2.00 ev and 2.25 ev have been plotted in Figs. 17 and 18 to indicate the sensitivity of the agreement between the theoretical curves and the experimental results to the choice of E_0. In comparing the position of the experimental points and the theoretical curves in Figs. 16–18, it should be noted that the same theoretical values have been used for all the curves and that the values of the parameters were not separately adjusted for each curve to give the best fit. The excellent agreement between the curves for widely different sample thicknesses therefore indicates the absence of appreciable systematic errors and is a valuable check on the significance of the results.

Although the shape of the transmission curves for times-of-flight greater than 20 microseconds/meter are well matched by theoretical curves for a negative level, assuming the above $1/v$ factor, a constant cross section of 15×10^{-24} cm^2/atom, and $-E_0=2.0$ ev, the actual relations may be somewhat different from this if the effect of the positive energy levels above 25 ev are considered. In Fig. 19 the experimental points for the 34.4 g/cm^2 sample for the high energy region are shown. An attempt was made to analyze this resonance by the standard procedure for positive resonances given above, but no satisfactory fit to the experimental results could be obtained. A theoretical transmission curve for a level with a resonant energy of $E_0=31.4$ ev and with a width of 37 ev is shown in Fig. 19 along with the experimental results. Even this very broad level would give a much sharper dip in the transmission than is actually observed. For this reason the broad shallow dip in the transmission in the region from 5 to 18

microseconds/meter is probably caused by several levels above 25 ev which may interfere with each other in such a manner that the net effect in the thermal region is negligible.

A rough estimate of the maximum effect that these positive levels could have on the calculation of the negative resonant energy can be made by using the fact that the transmission curve for the positive level always lies below the $1/v$ curve for $E<E_0$. If a straight line is drawn in Fig. 18 starting with $T=0.53$ at $t=0$ and passing somewhat above the experimental curve in the region of 35 microseconds/meter, this will represent the maximum effect that any positive levels could have on the transmission. Using this procedure a reasonable upper limit for the fraction of the total slope observed in the thermal region due to positive energy levels is of the order of 30 percent. If such an effect were assumed, the corresponding analysis for the negative level would give a value of the $1/v$ factor approximately 70 percent of that used in this analysis. The value of the negative resonance which would then be obtained would be about $-E_0=1.25$ ev. Probably the effect of the positive levels is smaller than this but this is an estimated maximum effect that could be expected.

In conclusion the results for the transmission measurements on mercury can be given with the following qualifications.

If the effect of the negative resonance level is assumed to be predominant for energies below 10 ev, then a good agreement is obtained with a Breit-Wigner one-level curve for

$$-E_0=(2.0\pm0.2)\text{ ev},\quad \Gamma\ll E_0,$$

$$\frac{\sigma_0\Gamma^2}{4E_0^{\frac{1}{2}}}=(64\pm3)\times10^{-24}(\text{ev})^{\frac{1}{2}}\text{ cm}^2/\text{atom},$$

$$\sigma_{\text{const}}=(15\pm1)\times10^{-24}\text{ cm}^2/\text{atom}.$$

In addition there is probably more than one level above 25 ev. The maximum possible effect that the positive levels could have on the negative resonance would be to change the resonant energy to -1.25 ev.

ACKNOWLEDGMENTS

The authors wish to express their appreciation of the active interest taken in this problem by Professor J. R. Dunning without whose active interest and stimulating discussion the investigations could not have been carried out. We also wish to thank Dr. W. E. Lamb and Mr. J. G. Beckerley for the help received in the discussion of some of the problems involved, and to thank the United States Indium Corporation for the loan of the thick indium sample. The Ernest Kempton Adams Fund has also aided materially in carrying out this research.